

Coupled-mode theory for general free-space resonant scattering of waves

Rafif E. Hamam, Aristeidis Karalis, J. D. Joannopoulos, and Marin Soljačić

Center for Materials Science and Engineering and Research Laboratory of Electronics, Massachusetts Institute of Technology,
Cambridge, Massachusetts 02139, USA

(Received 26 December 2006; published 2 May 2007)

We present a universal coupled-mode-theory treatment of free-space scattering of waves from resonant objects. The range of applicability of the presented approach is fairly broad: it can be used for almost any linear wave system, as long as the resonant scatterer has either three-dimensional (3D) spherical or 2D cylindrical symmetry, or else is sufficiently smaller than the resonant wavelength of the incident wave. The presented framework, while being intuitive and analytically simple, can nevertheless provide quantitatively very accurate modeling of scattering cross sections, absorption cross sections, and many other quantities of interest. We illustrate this approach by showing how it applies to the particular examples of scattering of light from spherically symmetric resonant objects and atoms, and scattering of neutrons off nuclei.

DOI: [10.1103/PhysRevA.75.053801](https://doi.org/10.1103/PhysRevA.75.053801)

PACS number(s): 42.25.Fx, 03.65.Nk

Coupled-mode theory [1] (CMT) has been tremendously successful in modeling a wide variety of systems that can entail any number of resonant objects weakly coupled to each other and/or to any number of incoming and outgoing ports. As long as the couplings are weak and the resonances are well defined, CMT provides an extraordinarily simple and intuitive, yet very accurate, analytical framework for modeling resonant behavior of complex systems whose more exact models can often be quite involved. Some examples of systems where CMT is being widely and successfully explored include optical waveguides and cavities, electronic resonant circuits, and coupled mechanical resonances. In this work, we show that the resonant scattering of freely propagating waves from resonant objects of two-dimensional (2D) cylindrical or 3D spherical symmetry can also be very accurately modeled using very simple CMT analytical expressions; the resonant objects can themselves entail more than one weakly coupled resonance. This technique can also often be used to analyze scattering from pointlike objects (i.e., objects much smaller than the incident wavelength), even when their substructure does not strictly obey 2D cylindrical or 3D spherical symmetry. Our approach can be applied to almost any free-space wave system. We illustrate it by modeling three well-known resonant scattering systems: scattering of light from spherically symmetric resonant objects, scattering of light from atoms (resonance fluorescence), and quantum-mechanical scattering of neutrons off nuclei.

Briefly, the general outline of our approach is as follows. First, one exploits the spherical (cylindrical) symmetry of the problem by placing the resonant scatterer at the origin, and decomposing the incoming wave into a discrete set of spherical (cylindrical) modes. Only a subset of these free-space modes will have the same angular symmetry as the dominant radiating modes of the scatterer, thus being able to couple with them. Second, we identify those free-space spherical (cylindrical) modes that are capable of coupling to the scatterer as the “ports” for the CMT framework: in practice, there will typically be only very few such modes. Next, the CMT coupling strength between the ports and the radiating modes of the scatterer is evaluated using the knowledge of the lifetimes of the resonances. Finally, the standard CMT framework is used to calculate powers that are dissipated

and/or scattered between the ports, from which various dissipation and/or scattering cross sections of interest can be trivially evaluated.

As a first illustrative example, we use the CMT formalism to analyze the specific case of an electromagnetic plane wave in air of wavelength $\lambda = 2\pi c/\omega$ and intensity I_0 incident on a spherically symmetric weakly absorbing resonant object of outermost radius b . The nature of the resonances in this system are long-lived whispering-gallery electromagnetic modes of the scatterer. Theoretical attempts [2,3] to understand quantitatively the scattering and absorption of light by small particles started almost a century ago with the Rayleigh approximation and the Mie theory. The Rayleigh treatment is limited to nonresonant scattering; the Mie solution to the problem is exact and applies to spheres of arbitrary size, but it is mainly a numerical solution that cannot be accomplished without resorting to a robust code. An empirical formula for the resonant light scattering from metal nanoparticles has been presented [4,5] based on Mie calculations. In contrast, we present here an analytical CMT treatment of the resonant light scattering from any spherically symmetric resonant object.

First, the scatterer is placed at the origin, and is described by a dielectric permittivity function $\varepsilon(r)$ and a magnetic permeability $\mu(r)$, both spherically symmetric. The resonant modes of the scatterer, $\vec{M}_{o,n\ell m}$, $\vec{M}_{e,n\ell m}$, $\vec{N}_{o,n\ell m}$, and $\vec{N}_{e,n\ell m}$, are generated from the solutions $\phi_{o,n\ell m} = R_\ell(k_n r) P_\ell^m(\cos \theta) \sin(m\varphi)$ and $\phi_{e,n\ell m} = R_\ell(k_n r) P_\ell^m(\cos \theta) \cos(m\varphi)$ of the scalar wave equation in spherical coordinates, as follows: $\vec{M}_{n\ell m} = \vec{\nabla} \times (\vec{r} \phi_{n\ell m})$ and $\vec{N}_{n\ell m} = (\vec{\nabla} \times \vec{M}_{n\ell m})/k_n$, $P_\ell^m(\cos \theta)$ being the associated Legendre function of the first kind, and k_n being the wave vector of the resonant mode. In the limit $r \gg b$, the radial part $R_\ell(k_n r)$ of the generating function $\phi_{n\ell m}$ behaves as the Hankel function of the first kind, $h_\ell^{(1)}(k_n r)$. Next, we expand the incident plane wave in terms of the free-space multipoles of radiation [2] $\vec{E}_{inc} = \vec{E}_0 e^{i(kz - \omega t)} = E_0 e^{-i\omega t} \sum_{\ell'=1}^{\infty} i^{\ell'} (2\ell' + 1) / [\ell'(\ell' + 1)] [\vec{M}'_{o,\ell'1} - i\vec{N}'_{e,\ell'1}]$, where $\vec{M}'_{o,\ell'1}$ and $\vec{N}'_{e,\ell'1}$ are vector spherical harmonics obtained from the generating function $\phi'_{o,\ell'1} = j_{\ell'}(kr) P_{\ell'}^1(\cos \theta) \left\{ \begin{smallmatrix} \sin \varphi \\ \cos \varphi \end{smallmatrix} \right\}$. Note that the major

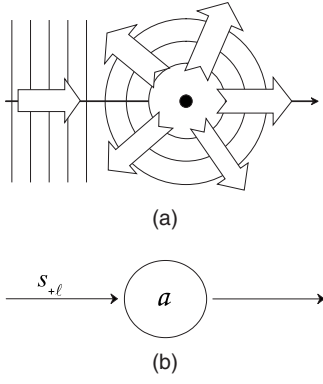


FIG. 1. Resonant scattering of a plane wave from a spherically symmetric scatterer. The top panel shows a schematic, and the bottom panel shows a coupled-mode-theory diagram. The resonant-mode amplitude is a , while $s_{+\ell}$ is the amplitude of the component of the incident wave that has the right symmetry to couple to the resonant mode of interest.

difference between the generating function ϕ of the resonant modes and the generating function ϕ' of the free-space multipoles lies in that the radial part of the latter is the spherical Bessel function $j_{\ell'}(kr)$, whereas the radial part of the former is some function $R_{\ell}(k_n r)$ that depends on the specific composition of the scatterer, and behaves as $h_{\ell}^{(1)}(k_n r)$ far from the scatterer's outermost radius b . The intensity I_0 of the incident plane wave is related to its electric field amplitude by $I_0 = (c\varepsilon_0/2)|E_0|^2$ where ε_0 is the permittivity of free space. The power $P^{(\ell')}$ incident onto the scatterer, and carried by the ℓ' component of the plane wave, is obtained by integrating the Poynting vector corresponding to the incident part of that component [$\propto h_{\ell'}^{(2)}(kr)$] over any closed surface enclosing the spherically symmetric resonant object; it is easiest to evaluate the surface integral over a very large sphere centered at the origin. The result is

$$P^{(\ell')} = \oint \vec{S} \cdot d\vec{a} = \frac{1}{4} \frac{\lambda^2}{2\pi} I_0 (2\ell' + 1). \quad (1)$$

If the incident wave has angular frequency $\omega = ck$ that is close to the resonance frequency ω_{res} of the scatterer in the TE mode $\vec{M}_{o,n\ell 1}$, then this wave will excite the mode $\vec{M}_{o,n\ell 1}$ with an amplitude proportional to α_{ℓ} , say. The scattered power P_{scat} is precisely the leaky power of this mode; it can be obtained by integrating the Poynting vector of this mode over any large spherical surface enclosing the scatterer. This results in $P_{scat} \propto |\alpha_{\ell}|^2$. Only the component proportional to $\vec{M}'_{o,\ell 1}$ in the plane wave, with $\ell' = \ell$, couples to the scatterer. Thus, we identify this mode with the $s_{+\ell}$ port of our CMT diagram shown in Fig. 1, and we associate the power $|s_{+\ell}|^2$ incident through this port with $P^{(\ell)}$: $|s_{+\ell}|^2 \equiv P^{(\ell)}$.

Let a represent the scatterer's resonant mode amplitude, normalized such that $|a|^2$ is equal to the energy in the resonant object. Let $1/\tau_{rad}$ and $1/\tau_{abs}$ denote the decay rates due to radiation and absorption, respectively. The corresponding quality factors are

$$Q_{rad} = \frac{\omega_{res} \tau_{rad}}{2} = \frac{\omega_{res} |a|^2}{P_{scat}} \quad (2)$$

and

$$Q_{abs} = \frac{\omega_{res} \tau_{abs}}{2} = \frac{\omega_{res} |a|^2}{P_{abs}}. \quad (3)$$

As long as Q_{rad} and Q_{abs} are sufficiently large, the CMT equation [1] satisfying energy conservation and time-reversal symmetry is

$$\frac{da}{dt} = -i\omega_{res} a - \left(\frac{1}{\tau_{rad}} + \frac{1}{\tau_{abs}} \right) a + \sqrt{\frac{2}{\tau_{rad}}} s_{+\ell} \quad (4)$$

$$\Rightarrow |a|^2 = \frac{\frac{2}{\tau_{rad}} |s_{+\ell}|^2}{(\omega - \omega_{res})^2 + \left(\frac{1}{\tau_{rad}} + \frac{1}{\tau_{abs}} \right)^2} \quad (5)$$

But, according to Eqs. (2) and (3), $P_{scat} = (2/\tau_{rad})|a|^2$ and $P_{abs} = (2/\tau_{abs})|a|^2$; therefore, using Eq. (1), the scattering and dissipation cross sections are given by

$$\sigma_{scat} \equiv \frac{P_{scat}}{I_0} = \frac{\left(\frac{1}{\tau_{rad}} \right)^2}{(\omega_{res} - \omega)^2 + \left(\frac{1}{\tau_{rad}} + \frac{1}{\tau_{abs}} \right)^2} (2\ell + 1) \frac{\lambda^2}{2\pi}, \quad (6)$$

$$\sigma_{abs} \equiv \frac{P_{abs}}{I_0} = \frac{\left(\frac{1}{\tau_{rad}} \right) \left(\frac{1}{\tau_{abs}} \right)}{(\omega_{res} - \omega)^2 + \left(\frac{1}{\tau_{rad}} + \frac{1}{\tau_{abs}} \right)^2} (2\ell + 1) \frac{\lambda^2}{2\pi}. \quad (7)$$

On resonance, the scattering and absorption cross sections are, respectively,

$$\sigma_{scat}^{res} = \frac{(1/\tau_{rad})^2}{(1/\tau_{rad} + 1/\tau_{abs})^2} (2\ell + 1) \frac{\lambda^2}{2\pi}, \quad (8)$$

$$\sigma_{abs}^{res} = \frac{(1/\tau_{rad})(1/\tau_{abs})}{(1/\tau_{rad} + 1/\tau_{abs})^2} (2\ell + 1) \frac{\lambda^2}{2\pi}. \quad (9)$$

The half widths at half maximum (HWHMs) of σ_{scat} and σ_{abs} are equal, and are given by

$$\Gamma_{scat}^{HWHM} = \Gamma_{abs}^{HWHM} = 1/\tau_{rad} + 1/\tau_{abs}. \quad (10)$$

Note that σ_{abs} is independent of the scatterer's outermost radius b ; when $b \ll \lambda$, the geometrical cross section πb^2 of the spherical object is much smaller than σ_{abs} ($\sim \lambda^2$). This reproduces the known fact [6] that a small resonant object can absorb much more than the light incident on it: $\sigma_{abs} \gg \pi b^2$.

To test the validity of our analytical formalism, we compare our CMT predictions to numerical results, in the special case of a homogeneous nonpermeable dielectric sphere of

radius b . In this case, the resonance frequency ω_{res} is given approximately by [5] $(c/b)z_\ell/n_{real}$ for $N_{e,n\ell 1}$ modes, and by $(c/b)z_{\ell-1}/n_{real}$ for $M_{o,n\ell 1}$ modes, z_ℓ being a zero of the Ricatti-Bessel function $u_\ell(z) \equiv zj_\ell(z)$. The quality factor for absorption is $Q_{abs} = \text{Re}[\varepsilon]/\kappa \text{Im}[\varepsilon] \approx n_{real}/2\kappa n_{im} \gg 1$ [7], assuming $n_{real} \gg n_{im}$, where ε is the dielectric function of the sphere, κ is the fraction of modal energy inside it, and $n_{real,im}$ are, respectively, the sphere's real and imaginary indices of refraction. In the limit of small nonpermeable spheres and large refractive index, the quality factor Q_{rad} for radiation is given analytically in Ref. [5]. When $Q_{rad} \gg 1$ and $Q_{abs} \gg 1$, the CMT approximation is valid.

Indeed, for a nonabsorptive sphere ($1/\tau_{abs}=0$), our analytical formula Eq. (9) reproduces the result $\sigma_{scat}^{res} = (2\ell+1)\lambda^2/2\pi$ obtained numerically by van de Hulst [3] for homogeneous dielectric spheres in the case $\omega b/c \ll 1$. Furthermore, we checked our analytical expressions against exact numerical results obtained from MIEPLOT [8] for the case $n_{real}=9$ and different ratios of Q_{rad}/Q_{abs} . As an illustration, the $n=2$ TE mode with $\omega_{res}b/c=0.4971$ has $Q_{rad}=3193$ and $\kappa=0.99$. The scattering cross sections are shown in Fig. 2(a) for the two cases $Q_{rad}/Q_{abs}=1$ and $Q_{rad}/Q_{abs}=2$, whereas the dissipation cross sections are shown in Fig. 2(b). In addition, a comparison between the analytical and numerical values of σ_{scat}^{res} , σ_{abs}^{res} , Γ_{scat}^{HWHM} , and Γ_{abs}^{HWHM} is presented in Table I, together with the relative errors, which are indeed very small, thus justifying the validity of the CMT approach. Lastly, we also verified our analytical expressions for homogeneous dielectric spheres with radius b both equal to and larger than λ , and obtained good agreement. However, in these cases, the nonresonant background contribution ($\sim \pi b^2$) to the cross section dominates over the resonant part ($\sim \lambda^2/2\pi$); thus, the resonant phenomenon, although well modeled, is not very pronounced.

In the above treatment of scattering from a spherically symmetric resonant object, the angular symmetry of the scatterer's resonant modes was exactly the same as that of the electric and magnetic multipoles of radiation, irrespective of the scatterer's size or radial composition. Hence, only one multipole component of the incident plane wave was scattered at resonance. Now, if we consider an arbitrary resonant scatterer (not necessarily of spherical or cylindrical symmetry), such that its size is much smaller than the wavelength of light illuminating it, then the far field of the resonant mode can be expanded in terms of electric and magnetic multipoles. However, given the small size of the resonant object, high-order multipoles contribute only a little to the far field, since those modes of large angular momentum are highly delocalized from the small region of space occupied by the object. Hence, the far field of the resonant mode can be well approximated in terms of the lowest few multipoles of radiation. Typically, for small enough objects, only one of these multipoles will be the dominant mode of radiation. Most often, this mode will be an electric dipole ($\ell=1$); if that one turns out to be prohibited, the dominant mode will be a magnetic dipole ($\ell=1$) or electric quadrupole ($\ell=2$), etc. In this case, our CMT formalism can also be applied, and the resonant cross sections are still given by Eq. (6) and Eq. (7), provided that they are multiplied by the squared modulus of

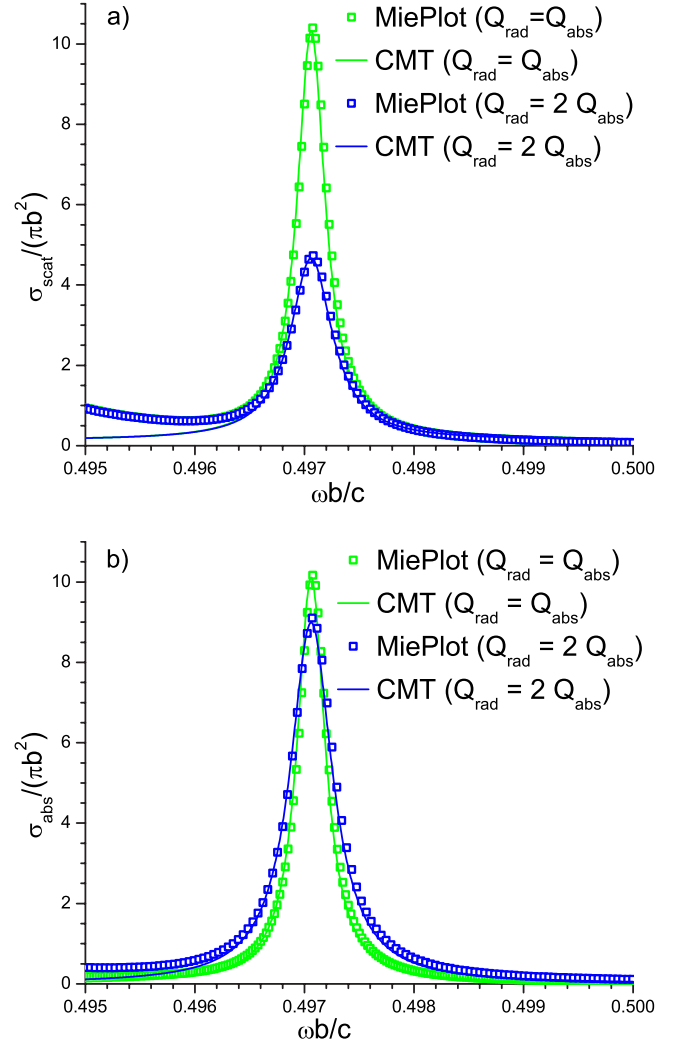


FIG. 2. (Color online) Comparison between MIEPLOT results and coupled-mode-theory predictions for a homogeneous nonpermeable dielectric sphere of radius b , in the cases $Q_{rad}=Q_{abs}$ and $Q_{rad}=2 Q_{abs}$. (a) Scattering and (b) absorption cross section.

the overlap between the dominant multipole mode of radiation and the incident plane wave. This takes into account the dependence of the resonant cross sections on the orientation of the incident plane wave, which is a consequence of the lack of spherical (cylindrical) symmetry of the scatterer. Examples of such objects include photonic microcavities, metallic nanoparticles, resonant radio antennas (whose size is

TABLE I. Cross-section peak values and HWHMs.

	$Q_{rad}=Q_{abs}$ ($n_{im}=0.00142$)			$Q_{rad}=2 Q_{abs}$ ($n_{im}=0.00284$)		
	MIEPLOT	CMT	Error	MIEPLOT	CMT	Error
$\sigma_{scat}^{res}/\pi b^2$	9.88	10.12	2.4%	4.6	4.5	2.2%
$\sigma_{diss}^{res}/\pi b^2$	10.03	10.12	0.9%	8.87	8.99	1.4%
$\Gamma_{scat}^{HWHM} b/c$	0.000153	0.000156	2.0%	0.000243	0.000233	4.0%
$\Gamma_{diss}^{HWHM} b/c$	0.000155	0.0001556	0.4%	0.000231	0.000233	0.9%

much smaller than the wavelength of the radio wave they couple to), atoms, etc.

As an example of such a system, we now consider the resonant scattering of radiation from atomic electrons. In this case, the scattering cross section can be found [9] phenomenologically from a simple classical model. The binding of an electron to its atom is represented by a spherically symmetric linear restoring force $-m_{electron}\omega_{res}^2\vec{r}$, where \vec{r} is the displacement of the electron from its equilibrium position, and ω_{res} is the resonant frequency of electronic oscillation. For an incident plane wave \vec{E}_{inc} of frequency ω , the electric force on the electron is $-e\vec{E}_{inc}$. Taking into account the small reactive effects of radiation, one can write an equation of motion for the electron (in the electric dipole approximation), and solve it for \vec{r} . A resistive term $m_{electron}(2/\tau_{abs})\dot{\vec{r}}$ is added to the equation of motion in order to account for dissipation. The scattering cross section can then be deduced from the expression of the radiated electric field of the oscillating dipole. Following this approach, one obtains [9]

$$\sigma_{scat} = \frac{3\lambda^2 \omega^4}{2\pi \omega_{res}^2} \frac{(2/\tau_{rad})^2}{(\omega_{res}^2 - \omega^2)^2 + \omega^2(2/\tau_{rad} + 2/\tau_{abs})^2} \quad (11)$$

where $1/\tau_{rad} \equiv \omega_{res}^2 \tau/2$ and $\tau \equiv \frac{2}{3}e^2/m_{electron}c^3$. For ω close to ω_{res} , this can be expanded to

$$\sigma_{scat} \approx \frac{3\lambda^2}{2\pi} \frac{(1/\tau_{rad})^2}{(\omega_{res} - \omega)^2 + (1/\tau_{rad} + 1/\tau_{abs})^2}. \quad (12)$$

In a similar fashion, one obtains

$$\sigma_{abs} \approx \frac{3\lambda^2}{2\pi} \frac{(1/\tau_{rad})(1/\tau_{abs})}{(\omega_{res} - \omega)^2 + (1/\tau_{rad} + 1/\tau_{abs})^2}. \quad (13)$$

Exactly the same expressions for σ_{scat} and σ_{abs} can alternatively be obtained using our CMT approach, as a special case of Eqs. (6) and (7), respectively, corresponding to $\ell=1$. The CMT treatment is still valid in this case, because the scatterer's resonant modes have the same symmetry as before, and hence the coupling of the incident plane wave to them is the same. The reason that the approach outlined above predicts only the $\ell=1$ case of the more general CMT result is that it represents the system by an oscillating electric dipole, and hence describes only the coupling of the electric dipole mode $\vec{N}_{e,n11}$, for which $\ell=1$.

So far, classical models of atomic transitions have succeeded in explaining only the electric dipole transition: magnetic dipole, electric quadrupole, and higher-order atomic transitions required a quantum mechanical analysis. In contrast, our phenomenological CMT formalism can be used to excellently reproduce quantum mechanical predictions for atomic transitions: electric or magnetic, dipole, quadrupole, or any of the higher-order ones.

Besides their applicability to resonance fluorescence, Eqs. (6) and (7) are also reminiscent of the Breit-Wigner (BW) formula for resonant scattering of neutrons from nuclei in compound nucleus reactions. This is not unexpected since "CMT-like" equations emerge throughout the derivation of the Breit-Wigner formula [10,11]. Using CMT formalism, we present here an alternative derivation of the formula BW

as an example of quantum mechanical resonant scattering. The nucleus (scatterer) is placed at the origin, and creates a localized central potential $U(r)$. The quasistationary states $\phi_{n\ell m} [= R_\ell(k_n r) P_\ell^m(\cos \theta) e^{im\varphi}]$ for a neutron in this potential have energies $E_{n\ell}$, with corresponding lifetimes $\tau_{n\ell}$. In the region outside the localized nucleus' potential, the radial part $R_\ell(k_n r)$ of the quasistationary states is given by the Hankel function of the first kind, $R_\ell(k_n r) \propto h_\ell^{(1)}(k_n r)$, since the potential is zero there. The incident neutron, of mass m_n , is assumed to be moving in the z direction, and is represented by a plane wave function $\psi_{inc} = A e^{i(kz - \omega t)}$, where A is determined by normalization. The neutron's wave function ψ_{inc} can be expanded in a basis consisting of the vacuum [$U(r)=0$] eigenstates in spherical coordinates, as follows: $\psi_{inc} = A \sum_{\ell'=0}^{\infty} i^{\ell'} (2\ell'+1) j_{\ell'}(kr) P_{\ell'}(\cos \theta)$. The probability current density associated with the ℓ' component of ψ_{inc} , $\psi_{inc}^{(\ell')}$, is $\vec{J}^{(\ell')}(\vec{r}, t) = (\hbar/m_n) \text{Im}[(\psi_{inc}^{(\ell')})^* \vec{\nabla} \psi_{inc}^{(\ell')}]$, and the corresponding probability per unit time is $p^{(\ell')} = \oint \vec{J}^{(\ell')} \cdot d\vec{a} = (2\ell'+1) \times (\pi \hbar / m_n V) (1/k)$, where $V = 1/|A|^2$ is the volume of the system. If the incident neutron has energy $E (= \hbar^2 k^2 / 2m_n)$ very close to the energy $E_{n\ell}$ of the quasistationary state $\phi_{n\ell m}$ of a neutron in the localized nuclear potential, then the only component of the incident neutron's wave function ψ_{inc} that couples to the nucleus is $\psi_{inc}^{(\ell)}$; this is because $\langle \phi_{n\ell m} | \psi_{inc} \rangle$ is nonzero only for $\ell = \ell'$ and $m=0$. Therefore, the probability per unit time that the neutron interacts with the nucleus is $p^{(\ell)}$, and we identify $p^{(\ell)}$ with $|s_{+\ell}|^2$ in our CMT formalism: $p^{(\ell)} \equiv |s_{+\ell}|^2$. Once the neutron couples resonantly with the nucleus, its wave function is given by the quasistationary state $\phi_{n\ell 0}$, with amplitude $a_{n\ell}$ satisfying the following CMT equation:

$$\frac{da_{n\ell}}{dt} = -i \frac{E_{n\ell}}{\hbar} a_{n\ell} - \frac{1}{\tau} a_{n\ell} + \sqrt{\frac{2}{\tau_{n\ell}}} s_{+\ell}, \quad (14)$$

where $1/\tau \equiv \Gamma/\hbar = \sum_j \Gamma_j/\hbar$ is the total rate of decay in all possible channels, and $1/\tau_{n\ell} \equiv \Gamma_i/\hbar$ is the decay rate in the same initial channel. In analogy with Eq. (5), we have $|a_{n\ell}|^2 = \{2\hbar \Gamma_i / [(E - E_{n\ell})^2 + \Gamma^2]\} |s_{+\ell}|^2$. The reaction rate at which the neutron's initial state $\psi_{inc}^{(\ell)}$ changes to $\psi_{inc}^{(f)}$ is $(2/\tau_f) |a_{n\ell}|^2 = \{4\Gamma_i \Gamma_f / [(E - E_{n\ell})^2 + \Gamma^2]\} |s_{+\ell}|^2$. This is also equal to the product of the flux $(1/V)(\hbar k/m_n)$ of incident neutrons and the cross section $\sigma(\psi_{inc}^{(\ell)} \rightarrow \text{channel } f)$ for decay into channel f . Therefore

$$\sigma(i \rightarrow f) = \frac{4\pi}{k^2} (2\ell + 1) \frac{\Gamma_i \Gamma_f}{(E - E_{n\ell})^2 + \Gamma^2}. \quad (15)$$

This result reproduces the well-known Breit-Wigner formula [12] obtained as a solution to a resonant scattering problem in quantum mechanics.

In conclusion, we have shown how to apply CMT to model resonant scattering of free-space waves from resonant objects. We illustrated this approach by applying it to three particular physical systems. In general, this approach could be useful for almost any free-space wave system, as long as the scatterer's resonances are well defined, and the scatterer is either sufficiently smaller than the wavelength or else has

2D cylindrical or 3D spherical symmetry. Moreover, if the scatterer has a few internal mutually interacting resonant modes (e.g., as in nonlinear dielectric spheres, or multilevel molecules with nonradiative coupling between the levels, etc.), the interaction between the modes can be easily modeled in the usual CMT way [1]. Incident wave packets that are localized in time and space could also be modeled, by decomposing them into their plane-wave components.

We would like to acknowledge helpful discussions with Professor Erich Ippen and Dr. Björn Maes. This work was supported in part by the Materials Research Science and Engineering Center Program of the National Science Foundation under Grant No. DMR 02-13282, the Army Research Office through the Institute for Soldier Nanotechnologies Contract No. DAAD-19-02-D-0002, and the U.S. Department of Energy under Grant No. DE-FG02-99ER45778.

-
- [1] H. A. Haus, *Waves and Fields in Optoelectronics* (Prentice-Hall, Englewood Cliffs, NJ, 1984).
- [2] J. A. Stratton, *Electromagnetic Theory* (McGraw-Hill, New York, 1941).
- [3] H. C. van de Hulst, *Light Scattering by Small Particles* (Dover, New York, 1981).
- [4] Hitoshi Kuwata *et al.*, *Appl. Phys. Lett.* **83**, 4625 (2003).
- [5] Roger G. Newton, *Scattering Theory of Waves and Particles* (Dover, New York, 2002).
- [6] Craig F. Bohren, *Am. J. Phys.* **51**, 323 (1983).
- [7] Marin Soljačić, Eleferios Lidorikis, Lene Vestergaard Hau, and J. D. Joannopoulos, *Phys. Rev. E* **71**, 026602 (2005).
- [8] P. Laven, Computer code MIEPLOT v3.4 (2006), <http://www.philiplaven.com/mieplot.htm>
- [9] J. D. Jackson, *Classical Electrodynamics* (Wiley, New York, 1999), pp. 766–768.
- [10] J-L. Basdevant, J. Rich, and M. Spiro, *Fundamentals in Nuclear Physics* (Springer, New York, 2005).
- [11] W. N. Cottingham and D. A. Greenwood, *An Introduction to Nuclear Physics* (Cambridge University Press, Cambridge, U.K., 2001).
- [12] J. J. Sakurai, *Modern Quantum Mechanics* (Addison-Wesley, Reading, MA, 1994).